Chinese Chemical Letters 36 (2025) 110298

Contents lists available at ScienceDirect

Chinese Chemical Letters

journal homepage: www.elsevier.com/locate/cclet

The controlled oxidation states of the $H_4PMo_{11}VO_{40}$ catalyst induced by plasma for the selective oxidation of methacrolein

Gang Hu [a], Chun Wang [a], Qinqin Wang [a], Mingyuan Zhu [b,*], Lihua Kang [a,*]

[a] School of Chemistry and Chemical Engineering/State Key Laboratory Incubation Base for Green Processing of Chemical Engineering, Shihezi University, Shihezi 832000, China

[b] College of Chemistry & Chemical Engineering, Yantai University, Yantai 264010, China

ARTICLE INFO

Article history:
Received 12 May 2024
Revised 17 July 2024
Accepted 26 July 2024
Available online 28 July 2024

Keywords:
Methacrolein
Methacrylic acid
Oxygen vacancy
Plasma
Catalyst
Dopant

ABSTRACT

In this paper, low-temperature dielectric-blocked discharge plasma (DBD) was employed for the first time to treat silica-doped $H_4PMo_{11}VO_{40}$ (HPAV) catalysts (DBD(Ar/x)-MF-Catal) and apply them in the catalytic methacrolein (MAL) selective oxidation to produce methacrylic acid (MAA). This work investigates in detail the controllable regulation of the concentration of oxidation states on silica-doped HPAV catalysts by adjusting the DBD discharge with controlled changes in voltage, current, treatment time, and treatment medium. It reports the intrinsic correlation between oxidation states and MAL oxidation performance. The research results indicated that the catalytic performance was related to the presence of oxygen vacancies and oxygen species (VO^{2+}), and are the main reason for the selective oxidation of MAL to MAA. Besides, the generation of oxygen vacancies and VO^{2+} altered localized electrons, which resulted in the easier activation of O_2. Theoretical calculations of DFT also proved the formation mechanism of oxygen vacancies and VO^{2+} and electron properties on high-performance polymers, which elucidated the intrinsic influence of catalyst components. The DBD(Ar/10)-MF-Catal catalysts with suitable VO^{2+} and oxygen vacancy concentrations exhibited the highest catalytic performance with 90% MAL conversion and 70% MAA selectivity and showed good stability (500 h).

Methacrylic acid (MAA) is a major chemical raw material serving as an important intermediate for the production of poly methyl methacrylate (PMMA), which is largely used in diverse industries including paints and coatings, electronics, as a modifier for PVC, and as bone inserts [1,2]. Up to now, the acetone-cyanohydrin (ACH) method has been the main conventional process to produce MAA. Nevertheless, the ACH method suffers from inherent drawbacks, such as high toxicity of the raw material HCN, strong acid corrosion of equipment, and the generation of a large amount of waste NH_4HSO_4, which have extremely restricted the MAA industrial development [3]. As a result, it is urgently necessary to develop a novel and green strategy to replace the ACH method. In recent years, two-step oxidation of isobutene to MAA has been universally proposed in many countries around the world, because this approach affords its advantages such as easy availability of raw materials, simplified process, low cost, and environmentally friendly, meanwhile, it can greatly improve the economic value of isobutene [4]. Unfortunately, methacrolein (MAL) is an important intermediate product in the two-step oxidation of isobutene, and it has widely reported that MAL selective oxidation is the key step for MAA manufacturing, which is the main technical barrier limiting the industrial application of this process route. Therefore, it is urgent to develop highly active catalysts for MAL selective oxidation, which is of great significance for the two-step oxidation of isobutene to MAA.

Until now, heteropolyacids (HPAs) have excellent characteristics such as Brønsted acidity, high proton mobility, and both electron donors and acceptors, making them green catalysts for efficiently catalyzing many organic reactions. Typically, it has been widely reported that HPAs can efficiently catalyze the MAL selective oxidation to MAA [5]. Among various widely developed HPAs, $H_4PMo_{11}VO_{40}$ (HPAV) delivers high proton conductivity and reversible multi-electron redox properties, which makes it the main catalyst for the gas-phase oxidation synthesis of MAA from MAL [6]. In particular, it has been extensively reported that HPAV catalysts modified with the antinuclear ions Cs^+ and NH_4^+ exhibit good redox properties. For example, Yu *et al.* obtained a series of catalysts by pretreating CsCu-(NH_4)HPAV with hydrogen and found that the oxidation state was a vital factor affecting their

* Corresponding authors.
E-mail addresses: zhuminyuan@shzu.edu.cn (M. Zhu), kanglihua@shzu.edu.cn (L. Kang).

https://doi.org/10.1016/j.cclet.2024.110298
1001-8417/

catalytic performance [6]. Besides, Zhang *et al*. found that calcination treatment can produce the oxidation state in CsCuFePMoV-NH, which was favorable for the MAL-MAA oxidation system [7]. In another research, Wang *et al.* synthesized polyamide-amine-$CsH_3PMo_{11}VO_{40}$ (PAMAM-CsPAV), which was treated at high temperature and formed more redox active sites (VO^{2+}), enhancing the MAL selective oxidation to produce MAA [8]. These research results indicated that the oxidized state in HPAV played a role of great importance in the MAL selective oxidation to produce MAA. Although many efforts have been devoted to applying different ways to regulate the oxidation state in HPAV compounds, there is still a great challenge to produce the oxidation state for the preparation of efficient and suitable catalysts, due to the limited knowledge about it. Up to now, the research on the oxidation state in HPAV catalysts is far from sufficient. Accordingly, to achieve the development and application of highly efficient and stable catalysts, it still is needed to get insight into the interrelationship between the oxidation state and the selectively catalytic MAL oxidation. The present studies confirm that the active vanadium oxide (VO^{2+}) and oxygen vacancy in HPAV catalysts are the main active oxide species in the oxidation of MAL for the synthesis of MAA. So far, there have been no reports on the controllable regulation and mechanism of vanadium oxide reduction and generation of oxygen vacancies ($VO_X \rightarrow VO^{2+} + O$) in HPAV catalysts, and it is believed that these researches are of great significance for the catalytic MAL oxidation to synthesize MAA. Therefore, it can be seen that developing catalysts with rich surface vanadium oxide (VO^{2+}) and oxygen vacancies has become an effective method to promote catalytic MAL oxidation to produce MAA.

As mentioned above, although various strategies have been employed to regulate the oxidation state of HPAV to produce catalysts for the MAL selective oxidation to high value-added MAA, their cognition is still not enough, and catalytic performance is not satisfactory. As a consequence, it is urgent to explore new strategies to endow heteropolyacids with a satisfactory oxidation state as catalysts for the MAL selective oxidation. Among various strategies, low-temperature dielectric barrier discharge (DBD) has attracted considerable attention [9,10], because it affords the inherent advantages: (1) Generation of a wide range of chemically reactive substances (including: high-energy electrons, free radical molecules, negative oxygen ions, ultraviolet photons, positive oxygen ions) and provision of energetic and excited state electrons by applying an electric field to a gas; (2) producing a large number of active sites by inelastic electron collisions; (3) triggering a series of physicochemical changes which are difficult to obtain by conventional methods, and so on [11,12]. Based on these advantages, some researchers have applied DBD to prepare highly efficient catalysts, such as, Bai *et al*. used plasma treatment of carbon paper electrodes to greatly improve the energy storage performance of ferrohydrogen batteries [13]; Guo *et al*. reported that oxygen plasma etching and modification of the surface of Co_3O_4 nanosheet arrays (NAs) at the cathode of lithium-oxygen batteries effectively improved the capacity of lithium-oxygen battery cathodes [14]. Among them, the most noteworthy is that DBD treatment can effectively regulate oxygen vacancy concentration and promote catalyst activity. For instance, Xu *et al*. activated the Mn/ZSM-5 catalysts by using DBD plasma and obtained the 7Mn/ZSM-5-CPM-DBD catalyst, which delivered a high activity for C_3H_6-SCR at ultra-low temperature. The characterizations confirmed that DBD plasma activation could generate higher active Mn species dispersion, larger pore size, more abundant oxygen vacancies, and less destructive to zeolite than traditional calcination activation [15]. In addition, Peng *et al*. synthesized the OV-Sb_2WO_6 photocatalyst after Sb_2WO_6 was treated by plasma under argon atmosphere. The photocatalytic experiments demonstrated that the as-obtained OV-Sb_2WO_6 achieved high activity and good stability, due to the introduction of oxygen vacancies after plasma treatment [16]. Other than, Jang *et al*. investigated the Ar or O_2 plasma treatment to modulate the oxygen vacancy concentration of the $MnCuO_x$-H catalyst to electrocatalyst the nitric acid reduction reaction to produce ammonia and achieved good catalytic results, this is attributed to the feature that the more oxygen vacancies formed from the plasma treatment could facilitate adsorption and weakening N-O bonds of NO_3 [17]. Additionally, Li *et al*. modulated its surface oxygen vacancies using plasma-induced oxidative desulfurization of a surface-reconstructed Mo-doped $W_{18}O_{49}$ catalyst thereby greatly improving the catalytic activity [18]. According to these researches, it can be inferred that plasma treatment can induce oxygen vacancies and alter metal oxide vacancy concentrations in HPAV catalysts to boost their catalytic performance. Therefore, the application of DBD treatment for HPAV to obtain catalysts is of great significance and promising.

Due to its discrete ionic structure and high proton mobility, HPAV exhibits disadvantages such as high solubility in water and other polar solvents and low specific surface area [19,20]. To overcome these shortcomings, much work has been done to combine HPAV with other materials [21-24]. Among them, nano-SiO_2 has many advantages as a HPAV dopant due to its unique properties such as cheap and easy availability, large specific surface area, and stable chemical properties [25-27]. Herein, based on the nano-SiO_2-doped HPAV catalysts that we studied earlier, we prepared the precursor catalyst (8($Cs(NH_4)_2PAV$)&4(Cs_3PAV)-NH_2-SiO_2 (abbreviations: Pre-Catal)) with Cs^+ and NH_4^+ modified HPAV growing on SiO_2 (15 ± 5 nm) *via* two-step *in-situ* molecular beam epitaxy. DBD was employed to treat roasted Pre-Catal (abbreviations: MF-Catal). During DBD discharge, the concentration of oxygen vacancies and metal oxide defects in DBD(y/x)-MF-Catal (y and x represent the gas medium and time of DBD activation treatment, respectively) was controlled by regulating voltage, current, processing time, and medium. Simultaneously, the effects of oxygen vacancies and metal oxidation states of catalysts for DBD treatment on catalytic performance and oxidation ability for the selective oxidation of MAL to MAA were further explored according to the experiments. Additionally, the formation of oxygen vacancies and VO^{2+} in HPAV and the intrinsic correlation between the effect of oxygen vacancies and VO^{2+} on catalysis were simulated and verified by DFT calculations. This work provides great theoretical significance and guiding value for the development of highly active, stable, and long-life catalysts for the MAL selective oxidation to prepare MAA.

The catalyst preparation and activation treatment process are shown in Fig. 1. Fig. 1a shows the preparation and roasting treatment process of the catalyst precursor. Fig. 1b shows the roasting catalyst modulating the oxygen vacancies and the metal oxidation state by DBD activation treatment. Specific details can be found in Supporting information.

The surface element composition and oxidation state of heteropolymer catalysts plays an important role in catalyzing the oxidation of MAL to MAA [28]. In order to investigate the effect of controllable oxidation state of DBD activation-treated catalysts on the intrinsic nature of the catalytic activity, surface elemental compositions and valence changes of Pre-Catal, MF-Catal and DBD activation-treated catalysts in Ar atmosphere were analyzed by XPS. The spectrums and surface analysis results of V $2P_{3/2}$, N 1s, O 1s and Mo 3d are recorded in Figs. 2a and b, Fig. S4 and Table S1 (Supporting information). From Fig. 2a and Table S1, it can be seen that the peaks appearing near 516.6 eV and 517.6 eV belong to V^{4+} and V^{5+}, respectively [29]. The V^{4+} and V^{5+} molar ratios of MF-Catal and DBD(Ar/x)-MF-Catal catalysts increased in the roasting and post-roasting DBD activation treatments, and the DBD(Ar/x)-MF-Catal catalysts showed an increasing trend in the V^{4+}/V^{5+} ratio with the increase of the DBD treatment time in

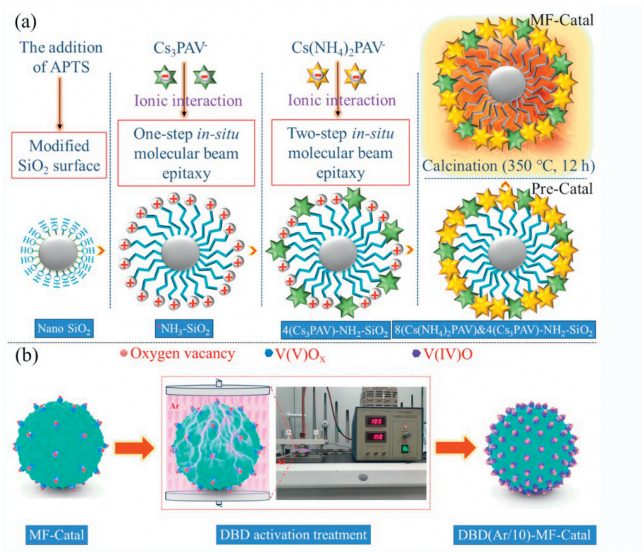

Fig. 1. Preparation process diagram of catalyst.

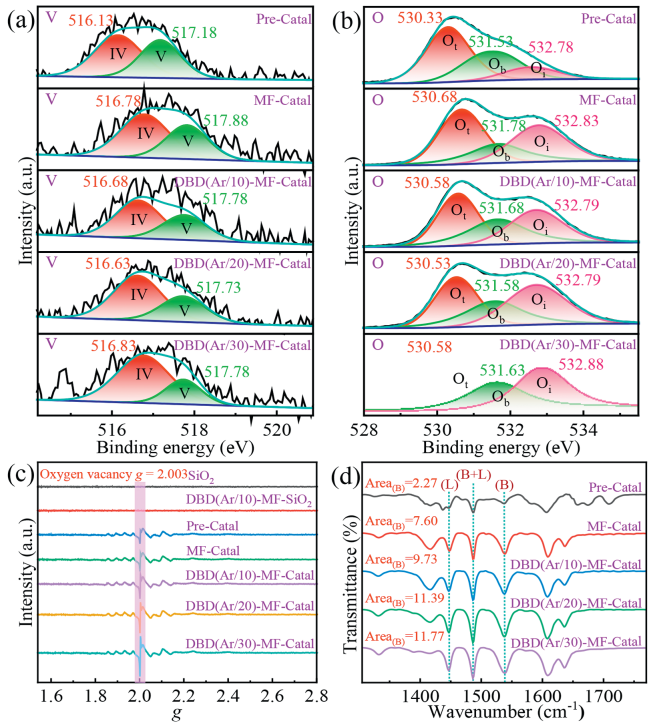

Fig. 2. (a, b) The narrow-scan XPS spectra of V and O of HPAV catalysts; O_t, O_b and O_i represent terminal oxygen, bridge oxygen and central oxygen in the HPAV catalysts, respectively. (c) EPR spectrum of SiO_2, DBD(Ar/10)-MF-SiO_2, Pre-Catal, MF-Catal and DBD(Ar/x)-MF-Catal catalysts. (d) Py-IR spectrum of Pre-Catal, MF-Catal and DBD(Ar/x)-MF-Catal catalysts.

Ar atmosphere, which indicated that the roasting and DBD activation contributed to the transformation of V^{5+} oxides to V^{4+} oxides in Pre-Catal catalyst. This is attributed to the self-reduction caused by the decomposition of organic matter and amino groups in the heat-treated heteropolymer compounds and DBD inelastic electron collisional activation treatments, which resulted in the formation of more VO^{2+} species in the secondary structure and interactions with the Keggin unit. The analysis of O 1s in Fig. 2b and Table S1 was obtained with spectra around 530.6, 531.7, and 532.8 eV for the three combined oxygen components of the HPAV heteropolymer compounds, corresponding to the surface terminal oxygens, bridging oxygens, and central oxygens (O_t, O_b and O_i), respectively [30]. The analytical effect of silica-oxygen is ignored here because they are similar species for comparison, whereas yet the silica remains in its pristine steady state during the roasting and activation treatments of DBD. The EPR tests of SiO_2 and DBD(Ar/10)-MF-SiO_2 in Fig. 2c gained this perspective. After the activation treatments of roasting and DBD, the fine peaks of oxygens changed significantly, the molar ratio of $O_t/(O_b+O_i)$ decreasing, and it significantly decreases with the increase of the activation time of the DBD treatment in argon, suggesting that the activation treatments of roasting and DBD altered the amount of O_t present on the surface. Combined with the accurate analysis of the fine spectra of V $2P_{3/2}$, N 1s (Fig. S4a in Supporting information), O 1s and Mo 3d (Fig. S4b in Supporting information) obtained, this is attributed to the easier cleavage of the V-O_t bonds in HPAV, this conclusion is also demonstrated in subsequent DFT calculations. It increases V-O_t fracture during roasting and DBD activation treatments, fragmenting into more lattice oxygen that spills over to form oxygen vacancies. Based on the detailed analyses of the V, N, O, and Mo elements on the surface of all catalysts, it is obvious that the peaks of each element are shifted towards higher binding energies. This indicates a change in the chemical environment of the surface elements, which is attributed to the activation of roasting and DBD contributed to the reduction and migration from the primary to the secondary structure of vanadium oxides in HPAV. During these activation processes, the V-O_t bond of the HPAV is broken and the V-O_t ligand (dotted oxygen) is oxidized to an O_2 molecule and escapes into the air, causing the reduction of V^{5+} and the formation of VO^{2+} and oxygen vacancies ($VO_X \rightarrow VO^{2+} + O$), which increases the concentration of VO^{2+} and oxygen vacancies (Fig. 1b). When analyzed in conjunction with the performance graphs of the activity tests, this may contribute to improving the catalytic activity of the oxidation reaction and is the main catalytically active site. These phenomena are in good agreement with the classical variants reported earlier [31].

EPR is an effective technique to characterize the changes in the elemental species morphology and relative oxygen vacancy concentrations for dopant and catalysts. The low-temperature EPR spectra of SiO_2, DBD(Ar/10)-MF-SiO_2, Pre-Catal, MF-Catal and DBD(Ar/x)-MF-Catal are shown in Fig. 2c. The ultrafine structure of vanadium (g-values: $g_{\parallel} = 1.932$, $g_{\perp} = 1.971$) indicates the presence of V(IV) form in Pre-Catal, MF-Catal and DBD(Ar/x)-MF-Catal catalysts [32]. The spectral intensities reveal that more V(IV) is present in MF-Catal and DBD(Ar/x)-MF-Catal than in Pre-Catal, and the intensity of V(IV) increases with the increase in the treatment time of DBD in Ar atmosphere, suggesting that the roasting and the activation treatment of DBD have led to an increase in the amount of VO^{2+}. EPR also determined the relative content of oxygen vacancies for SiO_2 and DBD(Ar/10)-MF-SiO_2, and pristine, roasted, and DBD-activated catalysts. Clearly, the SiO_2 and DBD(Ar/10)-MF-SiO_2 dopants do not show an oxygen vacancy signal of $g = 2.003$, indicating that the SiO_2 dopant is stable and maintains its original steady state in the roasting and activation treatment of DBD. While pre-Catal, MF-Catal and DBD(Ar/x)-MF-Catal show a significant oxygen vacancy signal of $g = 2.003$, which corresponds to the trapping of electron in the oxygen vacancies [33,34]. The oxygen vacancies concentration in the catalysts increased after the activation treatments of roasting and DBD, and the signal intensity was significantly enhanced with the increase of DBD treatment time in the Ar atmosphere compared to MF-Catal, which persuasively proved that the DBD activation treatments effectively increased the oxygen vacancies concentration in the DBD(Ar/x)-MF-Catal catalysts. This is because the DBD activation treatment induces the formation in HPAV of VO^{2+} and oxygen vacancies ($VO_X \rightarrow VO^{2+} + O$), which increases the concentration of VO^{2+} and oxygen vacancies in catalyst. These results are consistent with the XPS, UV–vis (Fig.

S8a in Supporting information) and Raman (Fig. S8b in Supporting information) results. They all indicate that the DBD treatments can change the concentrations of VO^{2+} and oxygen vacancies, and the DBD treatment of Ar can effectively and controllably regulate the concentrations of VO^{2+} and oxygen vacancies of the main catalytically active species. Many studies have shown that oxygen vacancies can improve catalytic performance by adsorbing oxygen and reducing reaction activation energy [35]. This may be the main reason for the increased activity of DBD activation treatment catalysts.

The synthesis of MAA by MAL oxidation requires both the oxidizing properties of the catalyst and its acidic properties for co-catalytic synthesis. Among them, the acidity of the catalyst plays an irreplaceable role in the carboxylation of aldehydes [36] and it is necessary to investigate the acidic properties of catalysts for the synthesis of MAA by MAL selective oxidation. The results of Py-IR and NH_3-TPD tests on the acidic properties of all catalysts are shown in Fig. 2d and Fig. S8c (Supporting information). In Fig. 2d, the Py-IR adsorption bands of all catalysts at 1450 cm^{-1}, 1540 cm^{-1} and 1488 cm^{-1} belong to Lewis, Bronsted and total adsorbed pyridine with acid-site coordination, respectively [37]. Comparing them, after roasting and DBD activation treatment, it was obtained that the Lewis, Bronsted and total acids of MF-Catal and DBD(Ar/x)-MF-Catal catalysts increased and were positively correlated with the treatment time of DBD. Such strong acidity of the catalysts is caused by the off-domains of the negative charge of the anion on the many oxygen atoms on the surface of the Keggin structure [38]. The roasting and DBD activation treatments promote the generation of VO^{2+} and oxygen vacancies (Figs. 2a–c), resulting in a larger space for the off-domains on the oxygen atoms, which reduces the charge density on the surface of the oxygen atoms in the Keggin structure, thereby increasing the mobility of the dihydrogen protons at the terminal oxygen of the heteropolymeric anions [8]. In addition, He *et al.* [37] reported that the presence of VO^{2+} species favors the generation of surface Lewis and Bronsted acid sites, which is consistent with the effective modulation of VO^{2+} concentrations by roasting and DBD activation in this study. NH_3-TPD further proves the validity of the acidic energy viewpoint of the catalyst (Fig. S8c in Supporting information).

The previous characterization shows that both roasting and DBD activation treatment can effectively promote the reduction of vanadium-oxygen species and the formation of oxygen vacancies ($VO_X \rightarrow VO^{2+} + O$), and the theoretical underpinnings of its formation are clearly important. The main active species VO^{2+} and oxygen vacancies are present in PAV^-, so the establishment and optimization of the above model of catalyzer is mainly to discuss the ion energy comparison of VO^{2+} and oxygen vacancy formation in PAV^-. The PAV^- model was executed using Gauss View 5.0 software, which systematically describes the mechanism of the PAV^- to form the major active sites of VO^{2+} and oxygen vacancies by density flooding theory (DFT), which is undoubtedly more convincing and supportive. The molecular energy calculations for the activation in PAV^- to break the V-O bond to form VO^{2+} and oxygen vacancy are shown in Fig. 3a. By assuming the breakage of different V-O bonds in PA^- ($PAV^-(D)$: V-O_t, $PAV^-(P)$: V-O_i, $PAV^-(Q1)$:V-O_{b1}, $PAV^-(Q2)$: V-O_{b2}, $PAV^-(Q3)$: V-O_{b3}, $PAV^-(Q4)$: V-O_{b4}) to form different stable ions containing VO^{2+} and oxygen vacancies, and by performing DFT analysis of the energies of different ions containing VO^{2+} and oxygen vacancies, it is obtained that the differential energy of breaking V-O_t bonds in PAV^- is the lowest and lower than other ion energies of containing VO^{2+} and oxygen vacancies ($PAV^-(D) < PAV^-(Q1) < PAV^-(P) < PAV^-(Q3) < PAV^-(Q4) < PAV^-(Q2)$). This suggests that the V-O_t bonds of PAV^- in the catalyst are more prone to break to form VO^{2+} and oxygen vacancies during roasting and DBD activation. This is consistent with the XPS characterization results, and further proves the correctness of the analytical results of V^{5+} reduction and oxygen vacancy formation

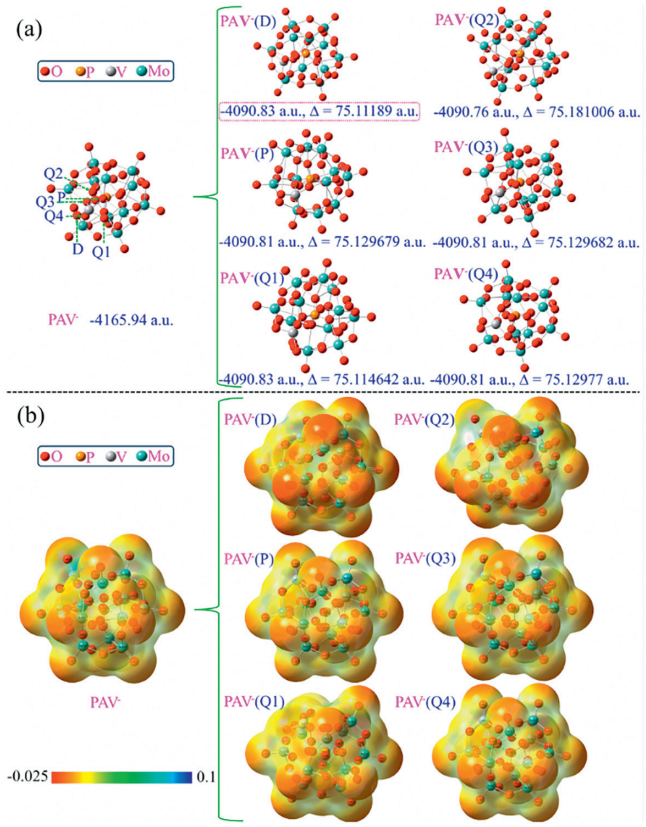

Fig. 3. (a) Molecular energy calculations for the PAV^- of breaking different V-O bond to form VO^{2+} and oxygen vacancy by activation. (b) Molecular electrostatic potentials on the van der Waals surfaces of the PAV^- of breaking different V-O bond to form VO^{2+} and oxygen vacancy by activation.

($VO_X \rightarrow VO^{2+} + O$) of PAV^- in the catalysts from theoretical calculations.

The catalytic oxidation of MAL to synthesize MAA must be accompanied by the transfer of electrons, and the surface charge distribution of catalyst clusters is undoubtedly important for the catalytic reaction. The effect of catalyst clusters forming different VO^{2+} and oxygen vacancy sites by activation on the catalytic activity must be related to the surface electronic properties, the molecular electrostatic potential of the van der Waals surface can well demonstrate the characteristics of charge distribution of different V-O bond breakage to form PAV^- containing different VO^{2+} and oxygen vacancy sites, and the results are shown in Fig. 3b. These electrostatic potential maps were plotted by setting the electron density to 0.001, with blue representing positively charged regions, red representing negatively charged regions, and darker red representing denser electron density. Compared to the PAV^- molecular electrostatic potential, the surface electron distribution of PAV^- containing different VO^{2+} and oxygen vacancy sites is significantly changed after activation. In the $PAV^-(D)$, $PAV^-(P)$, $PAV^-(Q1)$, $PAV^-(Q2)$, $PAV^-(Q3)$ and $PAV^-(Q4)$ plots, it can be observed that the red region of the $PAV^-(D)$ plot is more dense, which indicates that the electron density of the $PAV^-(D)$ region formed by V-O_t bond breaking is more denser, which makes it easier to transfer electrons during the catalytic reaction and exhibits stronger catalytic performance. Electron localization function (ELF can be found in Supporting information) further demonstrates that the formation of $PAV^-(D)$ by V-O_t bond breaking is more favorable for electron transfer in the reaction (Fig. S9 in Supporting information). To analyze more deeply and specifically the charge changes of vanadium and vanadium-adjacent oxygen atoms for different V-

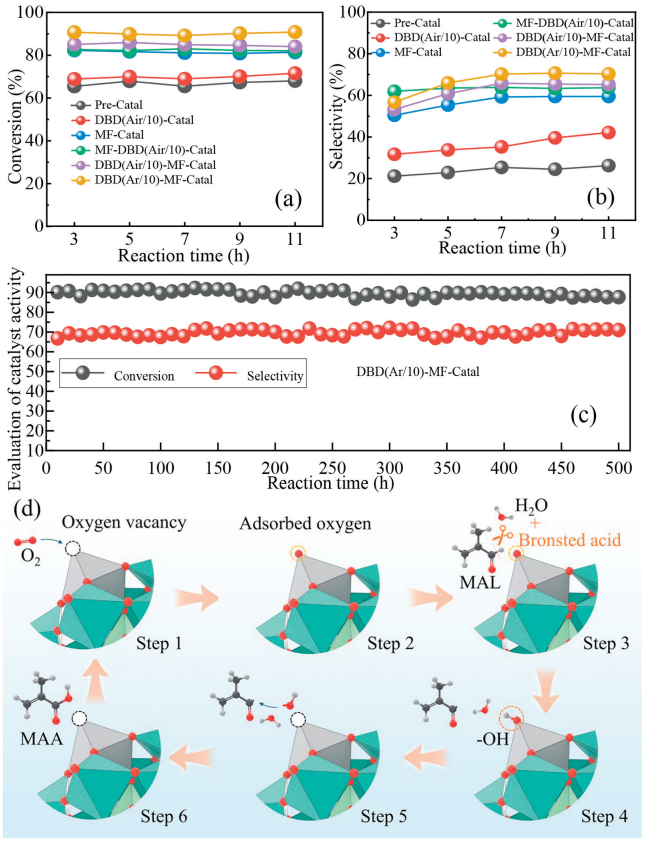

Fig. 4. Effect of different activation treatments on catalytic performance: (a) Conversion and (b) selectivity. (c) The long-time catalytic performance of DBD(Ar/10)-MF-Catal catalyst. (d) Catalytic mechanistic process of the oxygen vacancies of catalysts on the reaction of MAA synthesis by MAL oxidation.

O bond breaks to form PAV^- containing VO^{2+} and oxygen vacancy, the Maliken charges of the smallest units in the structure of PAV^- anions of containing VO^{2+} and oxygen vacancy have been calculated, and the results are shown in Table S3 (Supporting information). Table S3 lists in detail the Maliken charges of vanadium and vanadium-adjacent oxygen atoms in PAV^- containing different VO^{2+} and oxygen vacancy sites. Among them, the vanadium of PAV^-(D) formed by V-O_t bond breaking had the highest positive charge (1.546), indicating that the active sites formed by this group are more susceptible to transferring electrons and exhibit superior catalytic ability. This is a perfect fit with the above conclusion, which clearly and explicitly analyzes the effect of different V-O bond breakages of the PAV^- to form VO^{2+} and oxygen vacancy on catalytic electron transfer.

The oxidation state of HPAV is a key factor affecting the synthesis of MAA by MAL-catalyzed oxidation [6-8], and adjusting the oxidation state of the catalysts is an effective strategy to promote the MAA synthesis reaction. Roasting and DBD activation can effectively adjust the oxidation state of SiO_2-doped HPAV catalysts. The effects of these effective activation treatments on the catalytic activity are shown in Figs. 4a-c, and Figs. S10a and d (Supporting information). All catalyst evaluations were performed at 320 °C and GHSV of 1145 h^{-1}. Obtained from Figs. 4a and b, the conversion and selectivity of Pre-Catal and DBD(Air/10)-Catal catalysts without roasting activation treatment are relatively low. After the roasting activation treatment, the catalytic activity after roasting was improved to some extent. It was obtained by the test evaluation of the activity that the DBD(Ar/10)-MF-Catal catalyst with roasting in air first and DBD activation treatment afterward had the best activity, with 90% conversion and 70% MAA selectivity. The high energy and excited state electrons provided by DBD activation treatment can well regulate the oxidation state of HPAV. This is attributed to the fact that the average electron energy for DBD excitation is 1–10 eV, which is the optimal range for exciting molecular and atomic species and breaking chemical bonds [39]. Figs. S10a and d explored the optimal conditions for DBD activation treatment of MF-Catal catalyst (these data on catalytic activity are obtained from the 10-h average of the reaction), and it was obtained that the current, voltage, and treatment time of DBD activation treatment increased from small to increase, the conversion of MAL was positively correlated with the increase, and the selectivity of MAA was first increased and then decreases. The best catalytic performance of DBD(Ar/10)-MF-Catal catalyst was obtained when the catalyst was treated at (100 V, 1.5 A) in the Ar atmosphere for 10 min. For 500 h of continuous reaction (Fig. 4c), the conversion had a slight decrease, and the selectivity remained relatively stable (it showed good catalytic performance and stability compared to previously reported loaded catalysts (Table S4 in Supporting information)). Stem from the results of this thesis, we deduced the mechanistic process of the reaction between the oxygen vacancies and VO^{2+} of HPAV catalyst to this reaction, and the results are shown in Fig. 4d. Step 1: Adsorption of O_2 by oxygen vacancies; Step 2: Activation of O_2 by oxygen vacancies to form lattice oxygen atoms; Step 3: Bronsted acid of catalyst and water opens the carbon-hydrogen bond of the reactant molecule MAL and forms free proton; Step 4: Free proton and lattice oxygen form the reactive intermediate •OH; Step 5: Carbon bonding to •OH forms carboxylate group; Step 6: De-attachment of MAA on the catalyst and reversion of the catalyst oxygen vacancies to their original state. Based on this analysis of the influence of the above optimization of activation treatment methods and treatment conditions on catalyst activity, and combined with the characterization and DFT calculation, the following results are obtained:

(1) The thermal activation treatment by roasting first led to the decomposition of APTA and partial decomposition of the amino group, which optimized the pore structure and HPAV crystal phase content of MF-Catal catalyst, reduced part of the V^{5+} in HPAV, and generated a certain concentration of VO^{2+} and oxygen-vacancy active sites ($VO_X \rightarrow VO^{2+} + O$). Then, after the activation of DBD in the Ar atmosphere for 10 min, the V^{5+} was further reduced, which gave the DBD(Ar/10)-MF-Catal catalyst the optimal concentration of VO^{2+} and oxygen vacancies in the catalytic active sites. The catalyst conversion and selectivity can be well improved, which makes it easier to obtain maximum active surface oxygen and accelerate the generation of carboxylic acid groups and electron transfer on the catalyst surface. This is attributed to the simultaneous occurrence of reduction and re-oxidation in the Keggin unit, and the rates of these two processes depend on the number of effective active sites, which are closely related to the contents of VO^{2+} and oxygen vacancies.

(2) The migration concentration of VO^{2+} to the secondary structure and the concentration of oxygen vacancies can affect the electronic atmosphere of the Keggin unit, promoting charge transfer to enhance the oxidation and re-reduction capacity of the active substances in the redox process, and thus altering their redox properties. This is due to the migration of the electron cloud in the Keggin unit as a result of the gain activation and loss to participate in the reaction of oxygen atoms involved in the reaction during the redox process. Suitable concentrations of VO^{2+} and oxygen vacancies accelerated the oxidation reaction of MAL and improved the selectivity of MAA.

(3) The activation treatment of DBD enhanced the acidity of the catalyst and promoted the carboxylation of the aldehyde group, which was favorable for the generation of the target product MAA.

(4) However, the over-activation treatment of DBD in an argon atmosphere makes the catalyst contain an excessive concentration of oxygen vacancies. Especially, when its concentration is too high, it greatly increases the ability to activate O_2 and the concentration of reactive oxygen species, so that the ability to trigger a high rate of redox cycling occurs under the same reaction conditions, and reactive oxygen of portion oxidizes MAL to CO, CO_2 and acetate, reducing the yield of the target product MAA.

In this study, the roasted SiO_2-doped HPAV catalysts were subjected to DBD activation treatment conditions to obtain a series of catalysts with controllable oxygen vacancies and metal oxidation states. The controlled modification of the oxygen vacancies and metal oxidation states of HPAV due to DBD treatment and its intrinsic linkage to catalyze MAL were systematically investigated. It was found that the high catalytic activity can be attributed to the generation of abundant surface VO^{2+} and oxygen vacancies by the DBD activation treatment, which improves the redox properties and decreases the charge density on the surface of oxygen atoms in the heteropolymeric structure. The decrease in charge density increased the off-domain and dihydrogen proton mobility of the oxygen atom at the end of the heteropoly anion and enhanced the surface acid sites of the catalyst. However, excessive concentration of oxygen vacancies leads to excessive oxidation and decreases the reaction selectivity. DFT calculations to verify the theoretical reduction of V^{5+} species and the formation process of oxygen vacancies demonstrated that V-O_t is more likely to break to form V^{4+} and oxygen vacancies. Its formation affects the distribution of the electron localization in the Keggin unit and leads to a weakening of the metal-oxygen bonding, which results in an easier transfer of electrons and an easier excitation of oxygen atoms. DBD excitation treatment of heteropolymeric species is an effective method to modulate redox properties and greatly improve the catalytic performance of SiO_2-doped HPAV catalysts, which develops a new activation treatment method for the synthesis of high-activity catalysts and has a broad application prospect.

Declaration of competing interest

The authors declare that they have no known competing financial interests or personal relationships that could have appeared to influence the work reported in this paper.

CRediT authorship contribution statement

Gang Hu: Writing – original draft, Investigation, Formal analysis. **Chun Wang:** Resources, Investigation. **Qinqin Wang:** Resources, Investigation, Conceptualization. **Mingyuan Zhu:** Resources, Investigation, Conceptualization. **Lihua Kang:** Supervision.

Acknowledgments

This work was financially supported by the Taishan Scholars Program of Shandong Province (No. tsqn202103051), the Science and Technology Project of Xinjiang Bingtuan Supported by the Central Government (No. 2022BC001), and the Project of Scientific Research in Shihezi University (No. CXFZ202205).

Supplementary materials

Supplementary material associated with this article can be found, in the online version, at doi:10.1016/j.cclet.2024.110298.

References

[1] M. Mahboub, J. Dubois, F. Cavani, et al., Chem. Soc. Rev. 47 (2018) 7703–7738.
[2] M. Yuan, D. Huang, Y. Zhao, Polymers 14 (2022) 2632.
[3] L. Zhou, X. Zeng, M. Qi, et al., Chem. Eng. Sci. 272 (2023) 118584.
[4] M. Sennerich, P. Weidler, B. Kraushaar, Catal. Commun. 141 (2020) 106016.
[5] L. Deusser, J. Petzoldt, J. Gaube, et al., Ind. Eng. Chem. Res. 37 (1998) 3230–3236.
[6] J. Yu, Y. Yang, Y. Chen, et al., Ind. Eng. Chem. Res. 61 (2022) 10014–10023.
[7] H. Zhang, R. Yan, L. Yang, et al., Ind. Eng. Chem. Res. 52 (2013) 4484–4490.
[8] B. Wang, Y. Li, Q. Zhu, et al., Catal. Sci. Technol. 13 (2023) 887–897.
[9] D. Wang, Y. Zou, L. Tao, et al., Chin. Chem. Lett. 30 (2019) 826–838.
[10] K. Li, J. Ji, Y. Gan, et al., Chin. Chem. Lett. 33 (2022) 434–437.
[11] D. Ray, P. Chawdhury, K. Bhargavi, et al., J. CO_2 Util. 44 (2021) 101400.
[12] X. Li, J. Zhang, F. Zhou, et al., Chin. J. Catal. 39 (2018) 1090–1098.
[13] C. Bai, F. Ning, S. Pan, et al., Chin. Chem. Lett. 33 (2022) 1095–1099.
[14] X. Guo, L. Xiao, P. Yan, et al., Chin. Chem. Lett. 32 (2021) 3491–3495.
[15] J. Xu, T. Tang, X. Sheng, et al., J. Environ. Chem. Eng. 10 (2022) 107009.
[16] Q. Peng, Q. Ruan, B. Wang, et al., Colloid. Surface. A 681 (2024) 132724.
[17] D. Jang, J. Maeng, J. Kim, et al., Appl. Surf. Sci. 610 (2023) 155521.
[18] J. Li, J. Xiong, H. Huang, et al., Sep. Purif. Technol. 318 (2023) 123948.
[19] J. Li, Z. Yang, S. Li, et al., Ind. Eng. Chem. Res. 82 (2020) 1–16.
[20] A. Popa, V. Sasca, O. Verdes, et al., Mater. Res. Bull. 50 (2014) 312–322.
[21] K. Nowińska, R. Fórmaniak, W. Kaleta, et al., Appl. Catal. A 256 (2003) 115–123.
[22] H. Kim, J. Jung, D. Park, et al., Appl. Catal. A 320 (2007) 159–165.
[23] H. Kim, J. Jung, D. Park, et al., Catal. Today 132 (2008) 58–62.
[24] H. Kim, J. Jung, S. Yeom, et al., J. Mol. Catal. A 248 (2006) 21–25.
[25] E. Rocchini, M. Vicario, J. Llorca, et al., J. Catal. 211 (2002) 407–421.
[26] R. Klaysri, V. Preechawan, N. Thammachai, et al., Mater. Chem. Phys. 211 (2018) 420–427.
[27] N. Hassan, A. Jalil, I. Hussain, et al., Chem. Eng. Process. 165 (2021) 108469.
[28] B. Wang, H. Dong, L. Lu, et al., Catalysts 11 (2021) 394.
[29] Y. Cao, L. Wang, L. Zhou, et al., Ind. Eng. Chem. Res. 56 (2017) 653–664.
[30] Y. Cao, L. Wang, B. Xu, et al., Chem. Eng. J. 334 (2018) 1657–1667.
[31] Y. Liu, S. Wang, Y. Li, et al., Appl. Catal. A 643 (2022) 118789.
[32] L. Zhou, L. Wang, S. Zhang, et al., J. Catal. 329 (2015) 431–440.
[33] R. Jia, Y. Wang, C. Ling, et al., ACS Catal. 10 (2020) 3533–3540.
[34] T. Wu, H. Zhao, X. Zhu, et al., Adv. Mater. 32 (2020) 2000299.
[35] Z. Li, Q. Yan, Q. Jiang, et al., Appl. Catal. B 269 (2020) 118827.
[36] S. Yasuda, A. Iwakura, J. Hirata, et al., Catal. Commun. 125 (2019) 43–47.
[37] J. He, Y. Liu, W. Chu, et al., Appl. Catal. A 556 (2018) 104–112.
[38] A. Kuvayskaya, S. Garcia, R. Mohseni, et al., Catal. Lett. 149 (2019) 1983–1990.
[39] B. Ashford, Y. Wang, C. Poh, et al., Appl. Catal. B 276 (2020) 119110.